

Supplementary Materials

Solid State and Solution Study on the Formation of Inorganic Anion Complexes with a Series of Tetrazine-Based Ligands

**Matteo Savastano ¹, Celeste García-Gallarín ², Claudia Giorgi ¹, Paola Gratteri ³,
Maria Dolores López de la Torre ², Carla Bazzicalupi ^{1,*}, Antonio Bianchi ^{1,*} and
Manuel Melguizo ^{2,*}**

¹ Department of Chemistry "Ugo Schiff", University of Florence, Via della Lastruccia, 3-13, 50019 Sesto Fiorentino, Italy; matteo.savastano@unifi.it (M.S.); claudia.giorgi@unifi.it (C.G.)

² Department of Inorganic and Organic Chemistry, University of Jaén, 23071 Jaén, Spain; cgarcia@ujaen.es (C.G.-G.); mdlopez@ujaen.es (M.D.L.d.I.T.)

³ Department of NEUROFARBA- Pharmaceutical and Nutraceutical section, and Laboratory of Molecular Modeling Cheminformatics & QSAR, University of Florence, Via Ugo Schiff 6, 50019 Sesto Fiorentino, Italy; paola.gratteri@unifi.it (P.G.)

* Correspondence: carla.bazzicalupi@unifi.it (C.B.); antonio.bianchi@unifi.it (A.B.); mmelgui@ujaen.es (M.M.); Tel.: +39-(0)5-5457-3286 (C.B.); +39-(0)5-5457-3254 (A.B.); 34-(0)9-5921-2742 (M.M.)

Table S1. Selected contacts (\AA) in the $\text{H}_2\text{L}3(\text{ClO}_4)_2 \cdot 2\text{H}_2\text{O}$ crystal structure. Esd in parentheses.

N1–C4	3.414(9)
O3–C5	3.36(1)
C8–O6	3.08(1)
C3–O5	3.306(8)
C6–O4	3.561(8)
O2–O3	2.843(7)
O1–O2	2.830(7)
H1–O2	1.98(7)

Table S2. Selected contacts (\AA) in the $\text{H}_2\text{L}4(\text{ClO}_4)_2 \cdot 2\text{H}_2\text{O}$ crystal structure. Esd in parentheses.

N5–O4	2.766(4)
O4–O11	2.832(4)
O4–O14	2.814(4)
O12–C15	3.171(4)
O12–C16	3.255(4)
O14–C8	3.208(5)
O13–C15	3.177(5)
O13–C2	3.387(5)
O14–C9	3.218(4)
C17–O23	3.172(4)
O3–C9	3.197(4)
O23–O3	2.939(4)
O22–C6	3.245(4)
O21–O3	2.847(4)
N6–O3	2.721(4)

Table S3. Selected contacts (\AA) in the $\text{H}_2\text{L3}(\text{PF}_6)_2$ crystal structure. Esd in parentheses.

C3–F1B/F1A	3.284(9)/3.32(1)
C6–F3B/F3A	3.37(1)/3.37(1)
C8–F3B/F3A	3.29(1)/3.39(1)
C7–F5B/F5A	3.05(1)/2.95(1)
C5–F5B/F5A	3.17(1)/3.09(1)
C3–F6B/F6A	3.172(7)/3.129(.008)
C8–F6B/F6A	3.266(8)/3.297(.009)

Table S4. Selected contacts (\AA) in the $\text{H}_2\text{L3}(\text{PF}_6)_2 \cdot 2\text{H}_2\text{O}$ crystal structure. Esd in parentheses.

C5–F2	3.308(5)
C8–F1	3.153(5)
C8–F6	3.162(5)
C4–F5	3.157(5)
C6–F3	3.269(5)

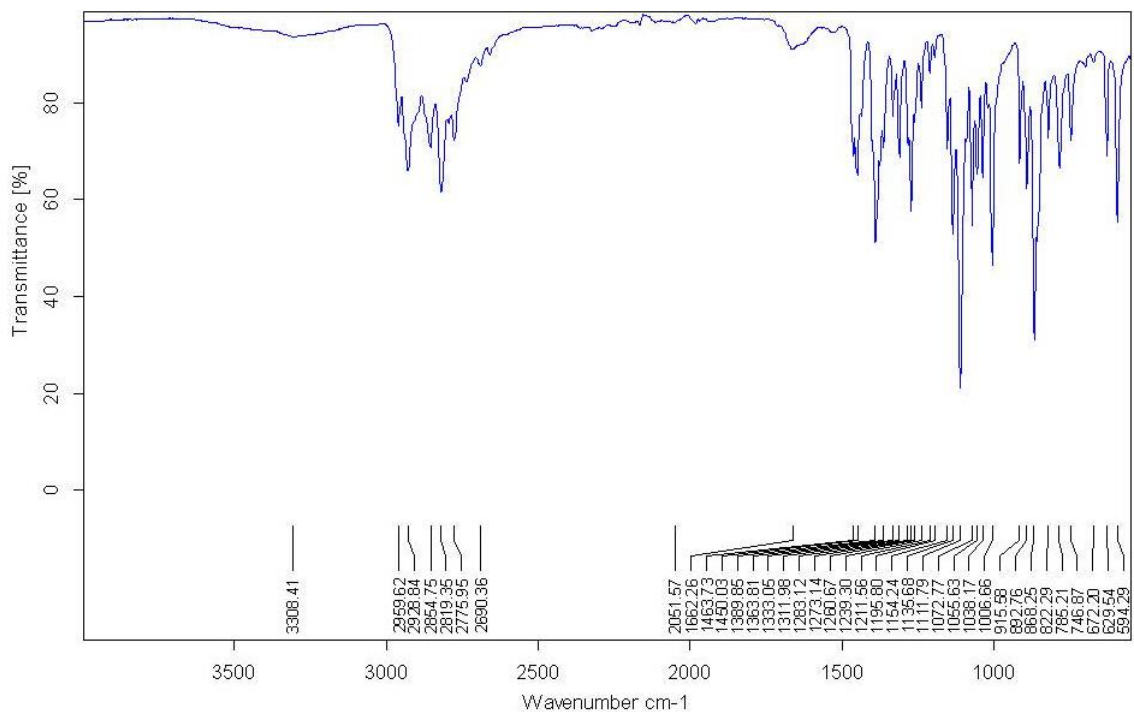


Figure S1. FTIR (ATR) of L3.

L3 / 1H-NMR

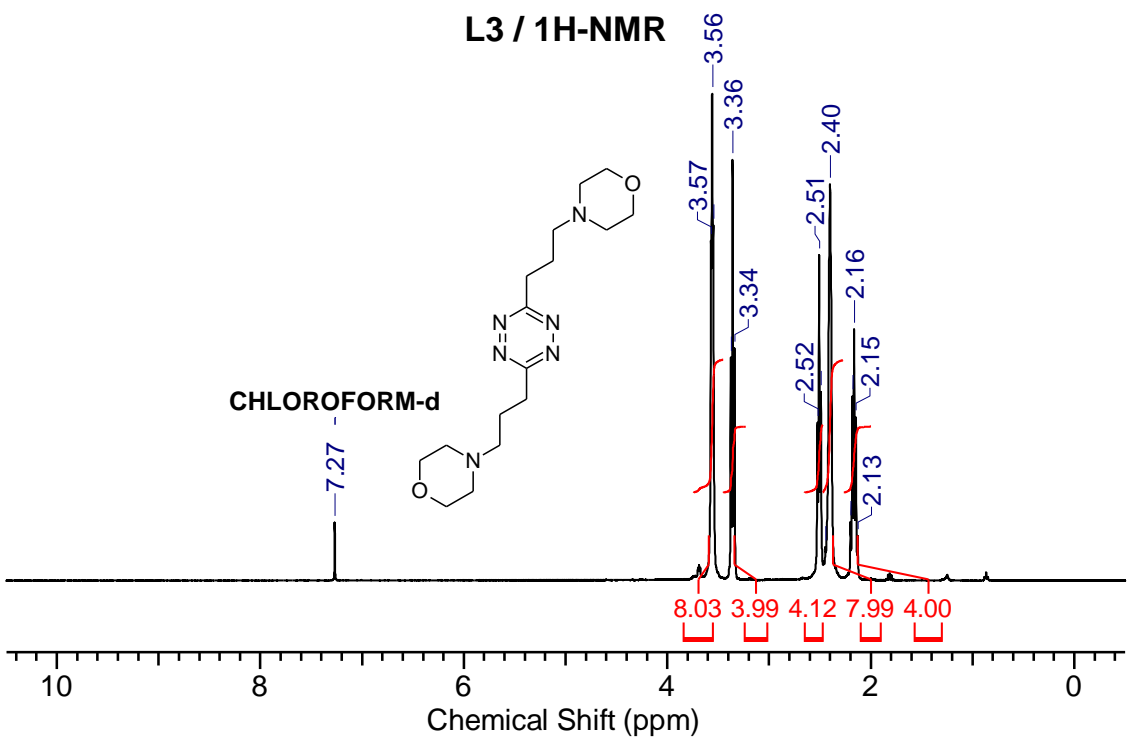


Figure S2. ¹H-NMR (CDCl_3 , 400 MHz) spectrum of L3.

L3 / ^{13}C -NMR

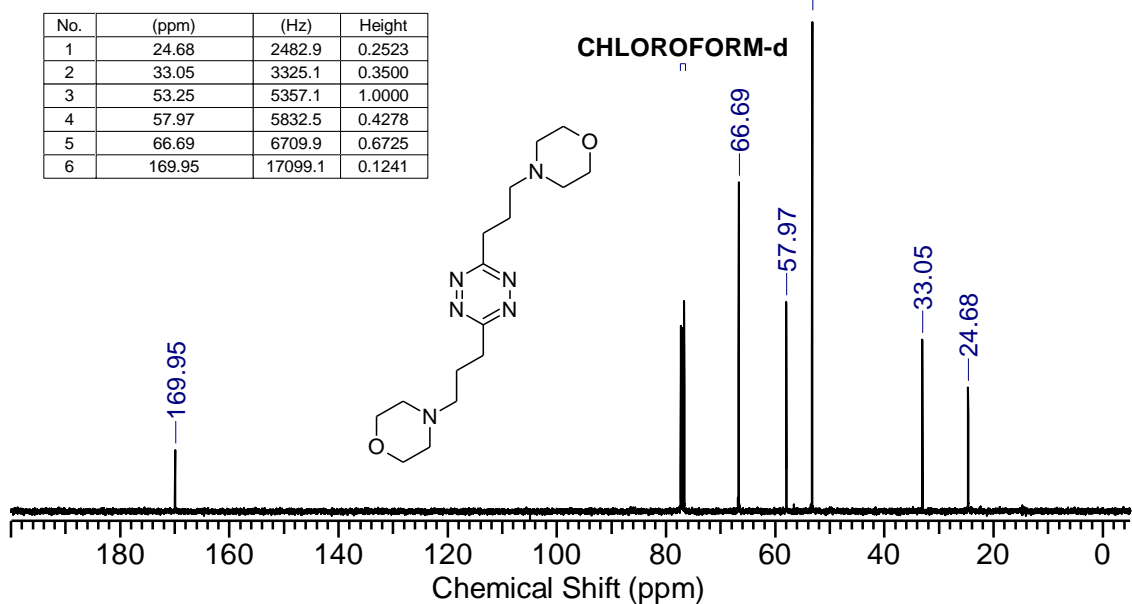


Figure S3. ^{13}C -NMR (CDCl_3 , 100 MHz) spectrum of L3.

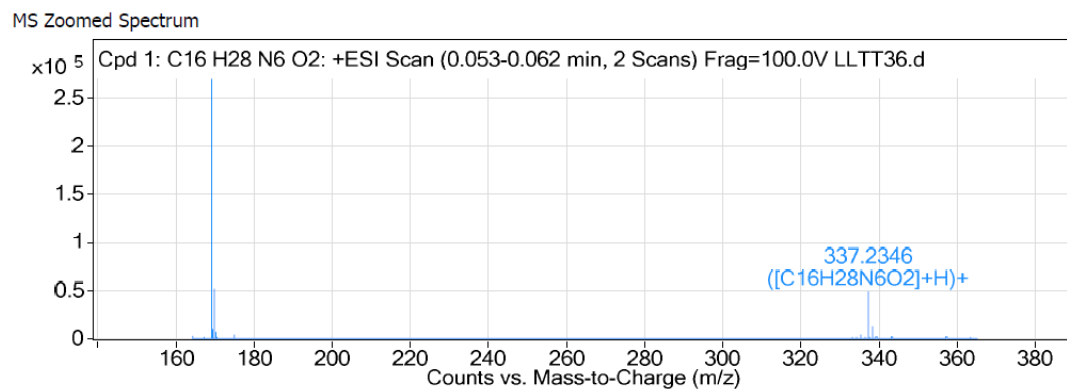


Figure S4. HRMS (Q-TOF/ESI) spectrum of L3.

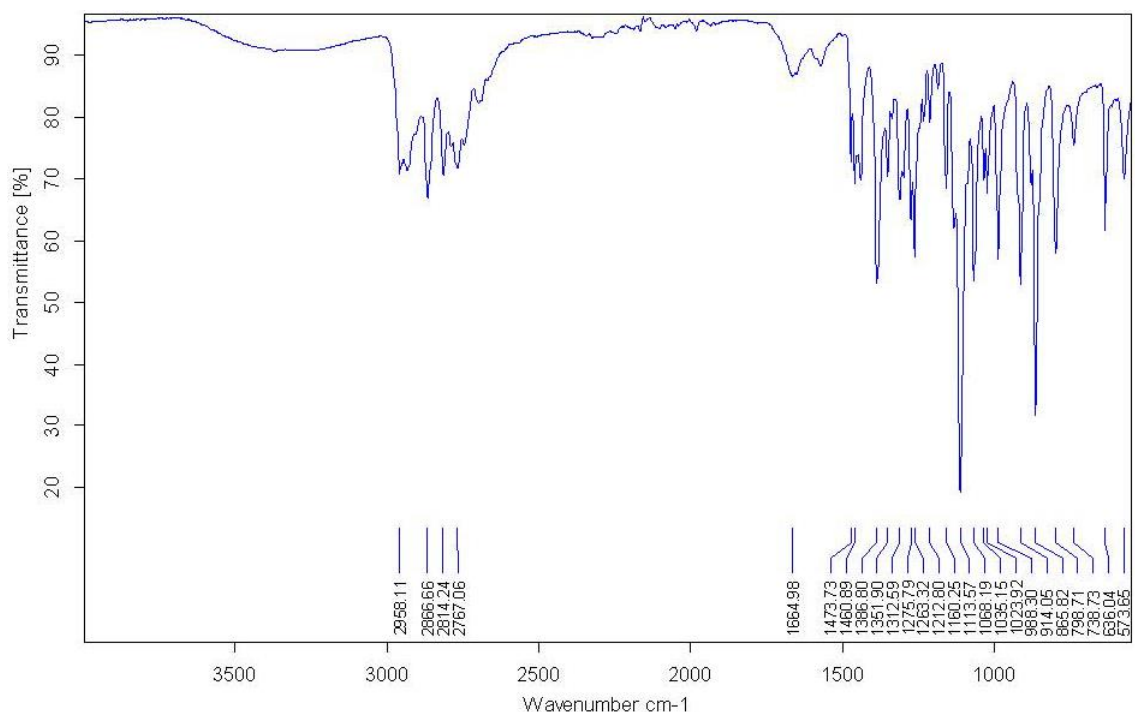


Figure S5. FTIR (ATR) of L4.

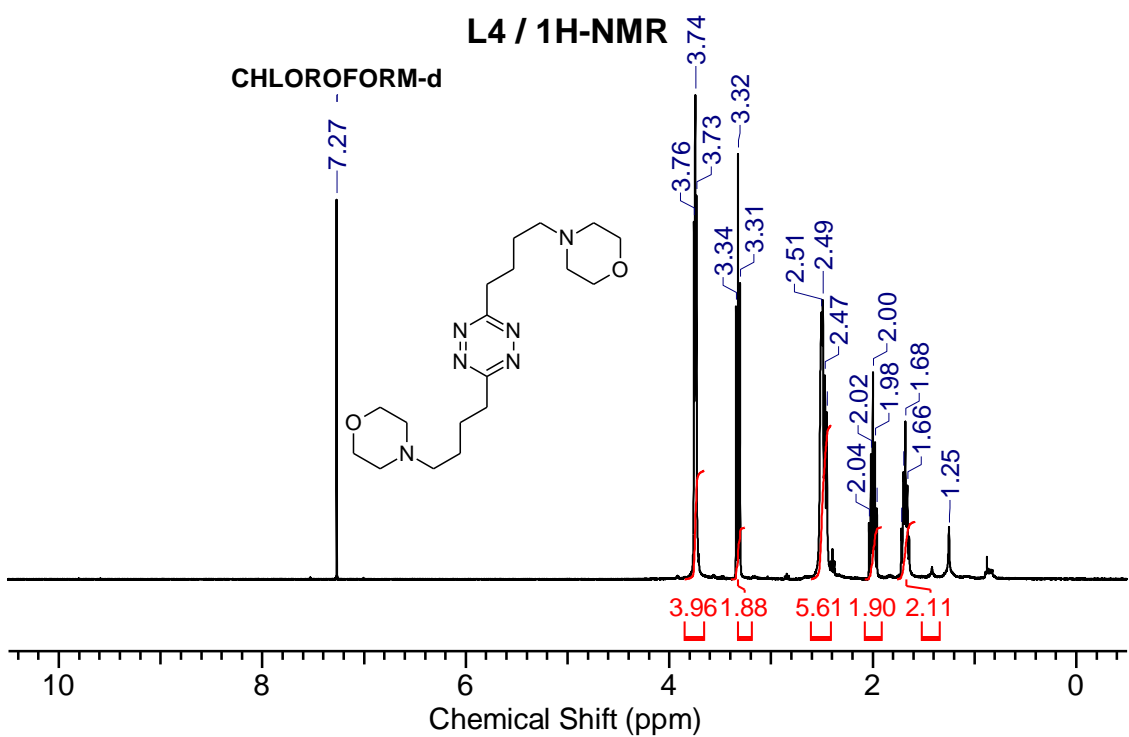


Figure S6. $^1\text{H-NMR}$ (CDCl_3 , 400 MHz) spectrum of L4.

L4 / ^{13}C -NMR

CHLOROFORM-d

No.	(ppm)	(Hz)	Height
1	25.63	2578.3	0.1498
2	25.87	2603.2	0.3525
3	34.45	3465.9	0.3813
4	53.52	5385.0	0.6271
5	58.31	5866.2	0.3138
6	66.57	6698.1	0.3316
7	169.91	17094.7	0.2276

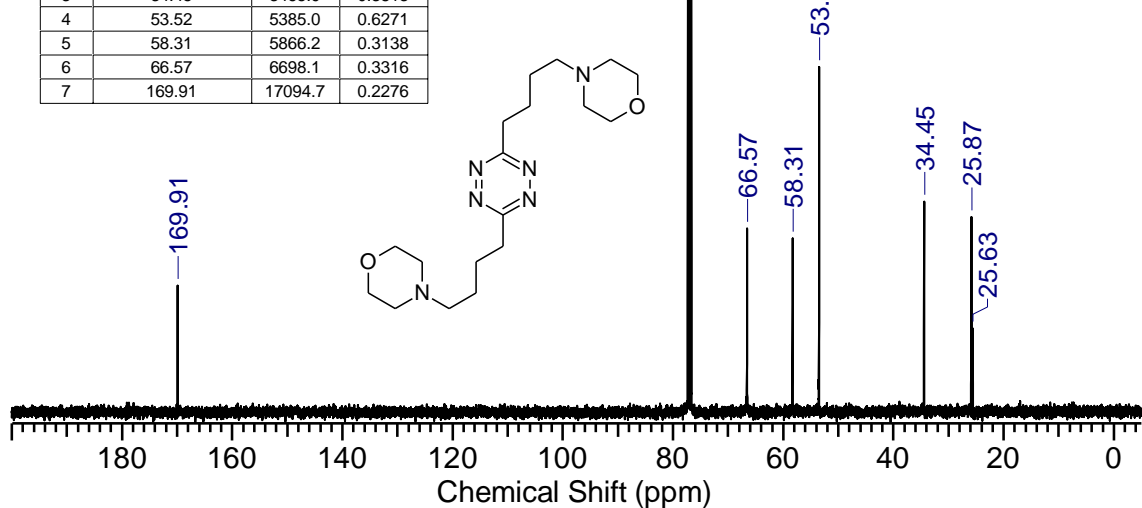


Figure S7. ^{13}C -NMR (CDCl_3 , 100 MHz) spectrum of L4.

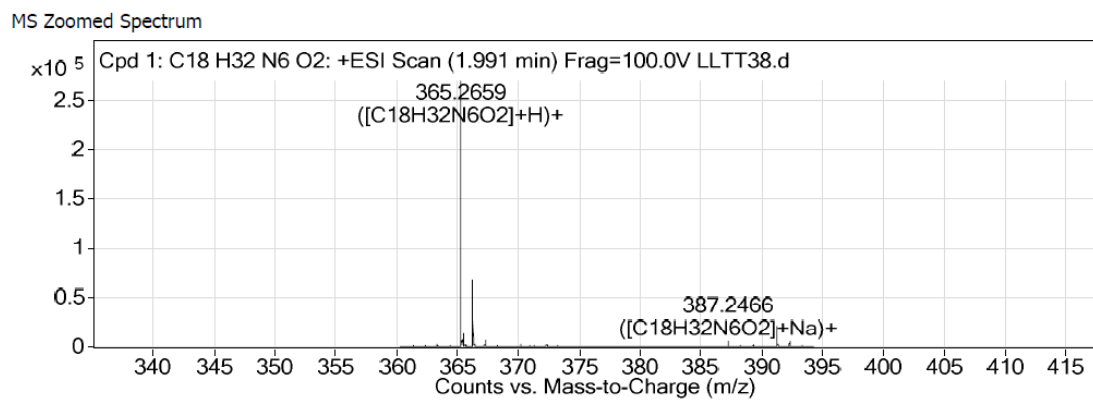


Figure S8. HRMS (Q-TOF/ESI) spectrum of L4.

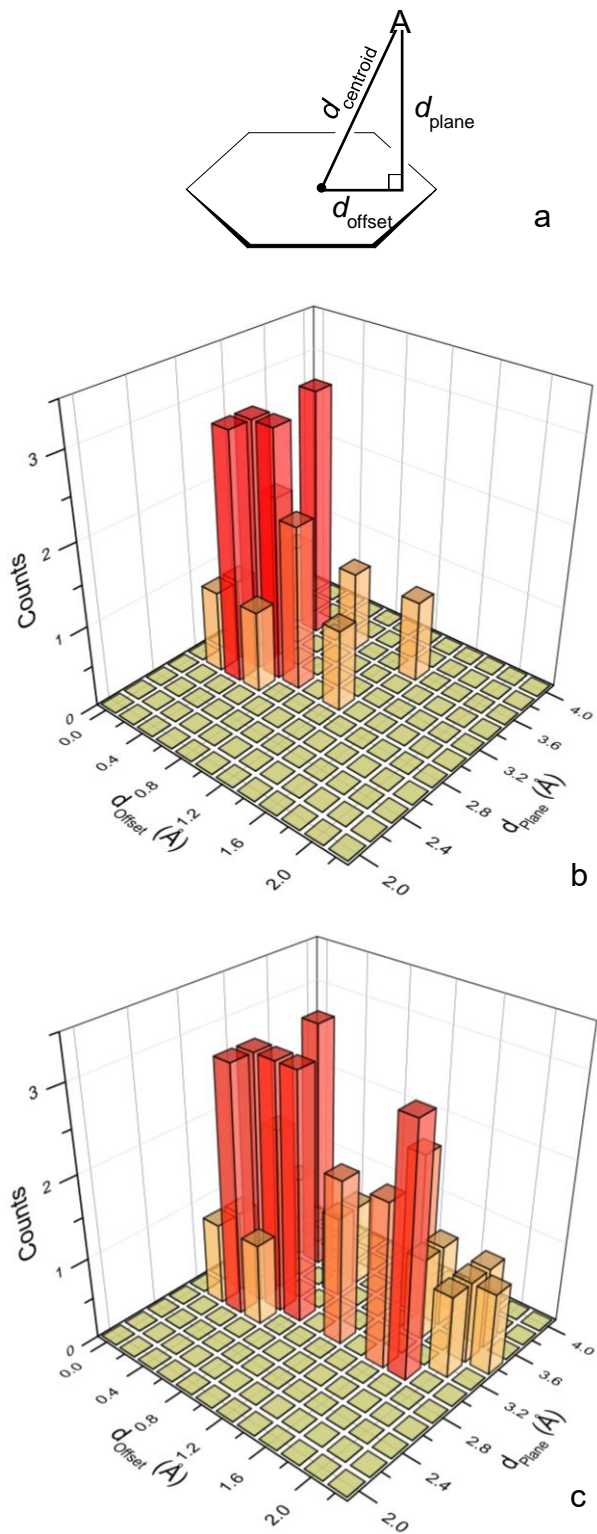


Figure S9. (a) Displacement of an atom A from the centre (centroid) of the tetrazine ring. (b) Frequency of shorter anion-ring contacts, for each anion, in the d_{plane} vs d_{offset} plane. (c) Frequency of all anion-ring contacts in the d_{plane} vs d_{offset} plane.

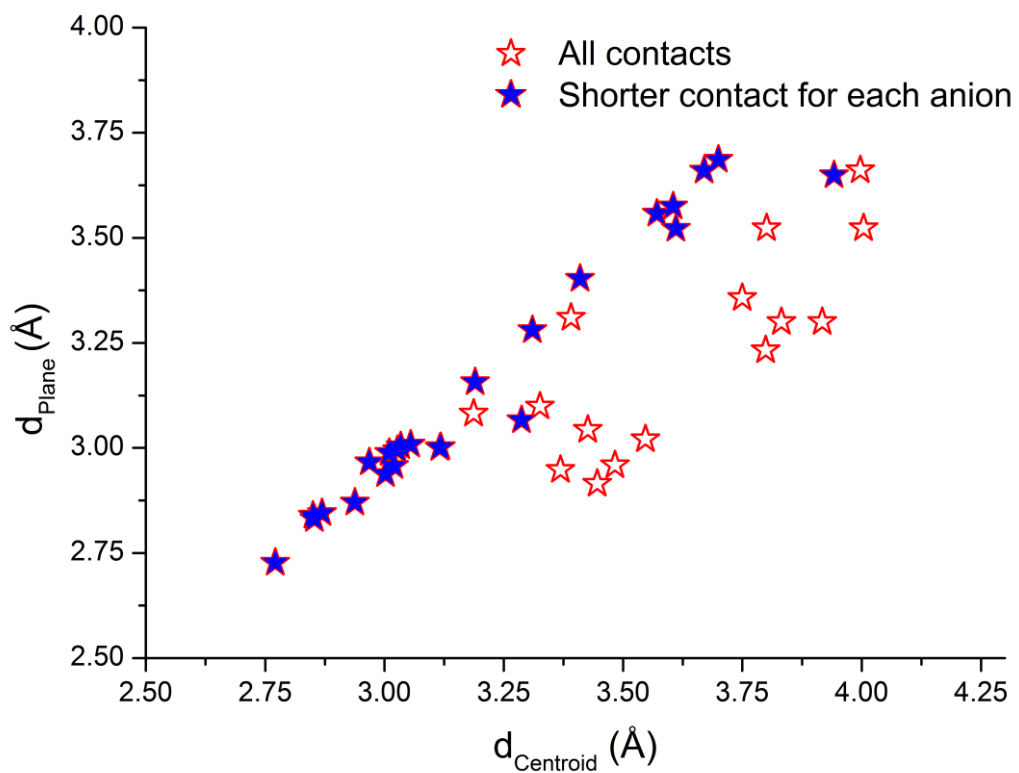


Figure S10. Correlation between d_{plane} and d_{centroid} distances in the crystal structures of L1-L4 anion complexes.

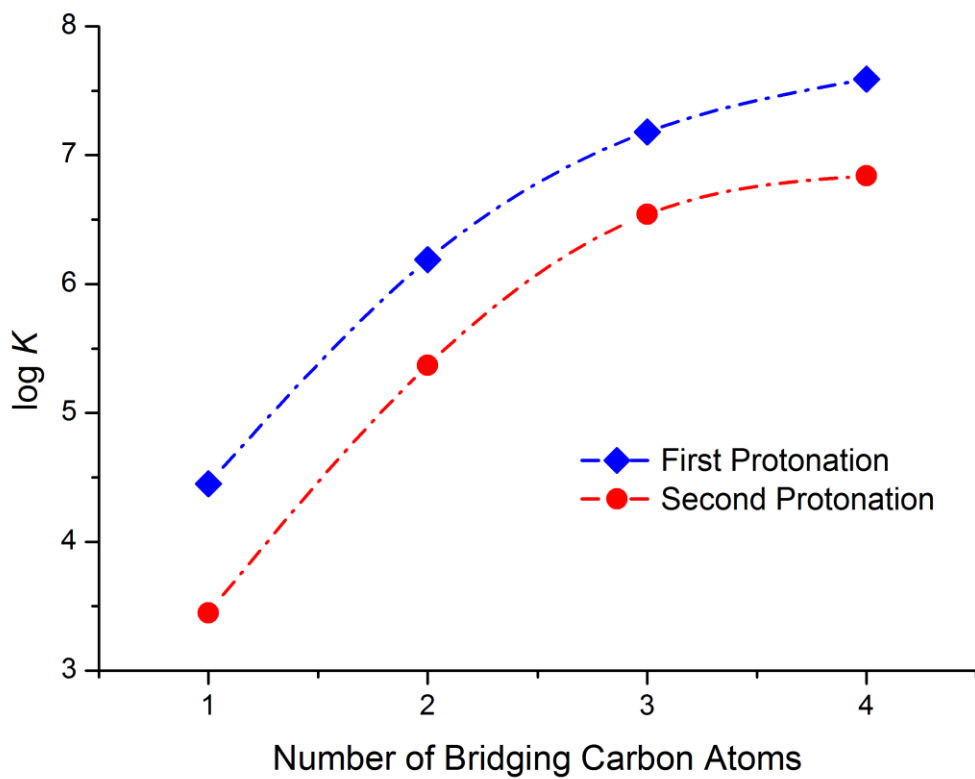


Figure S11. Hyperbolic fitting for the first and the second series of protonation constants ($\log K$) of L1-L4 ligands.

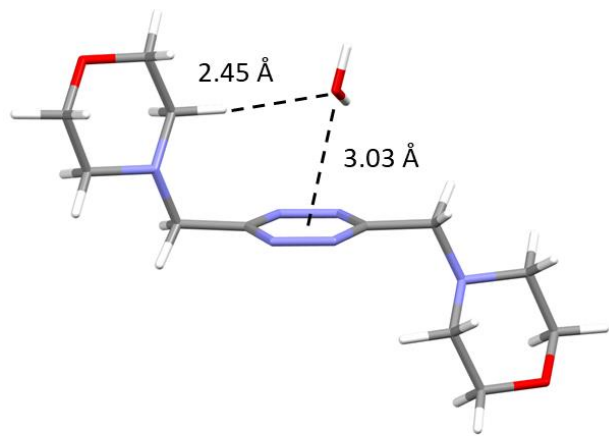


Figure S12. Calculated conformation for the [L1(H₂O)] adduct.

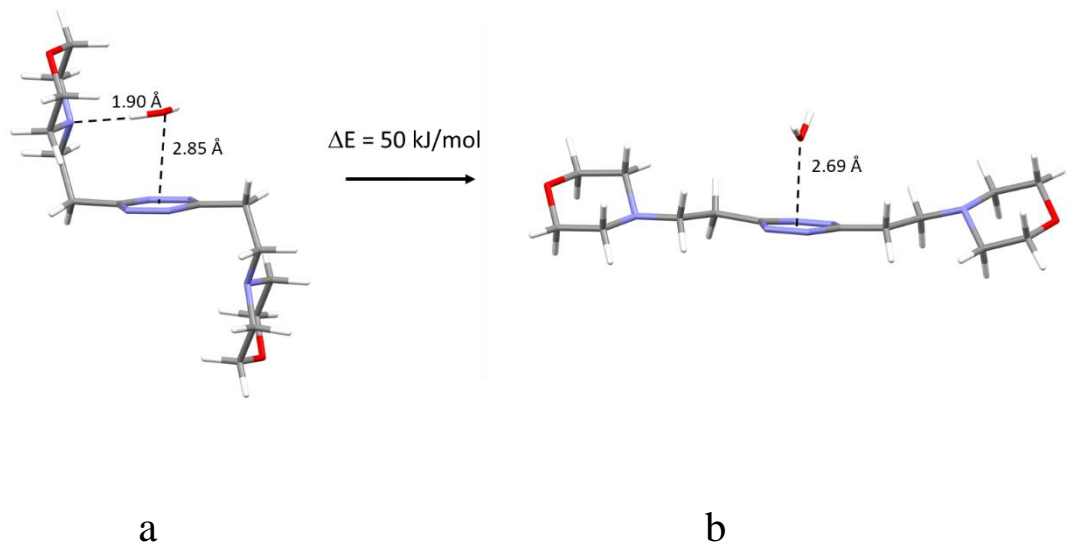


Figure S13. Calculated conformations for the [L2(H₂O)] adduct: a) chair conformation, b) planar conformation.

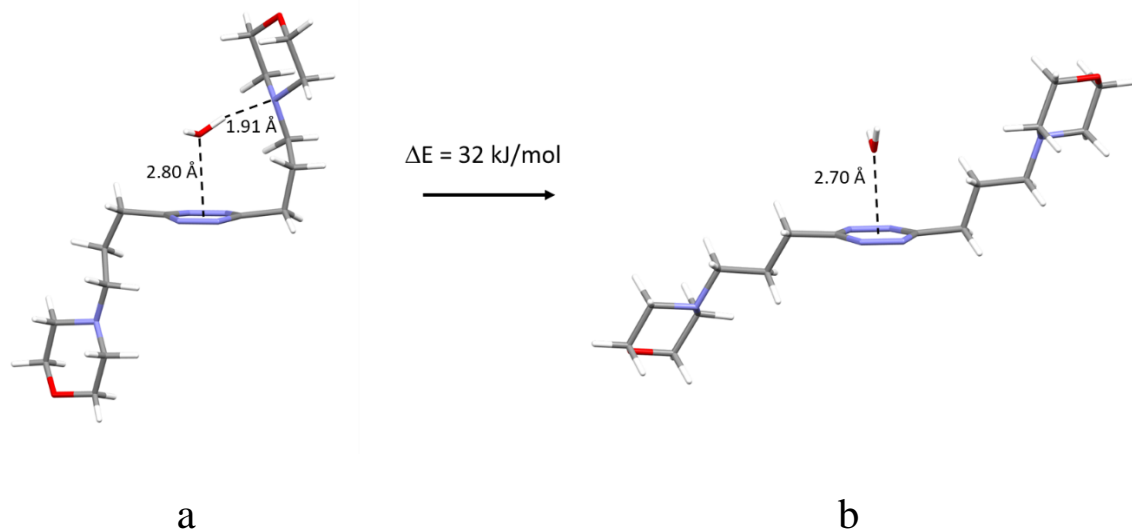


Figure S14. Calculated conformations for the $[L3(H_2O)]$ adduct: a) chair conformation, b) planar conformation.

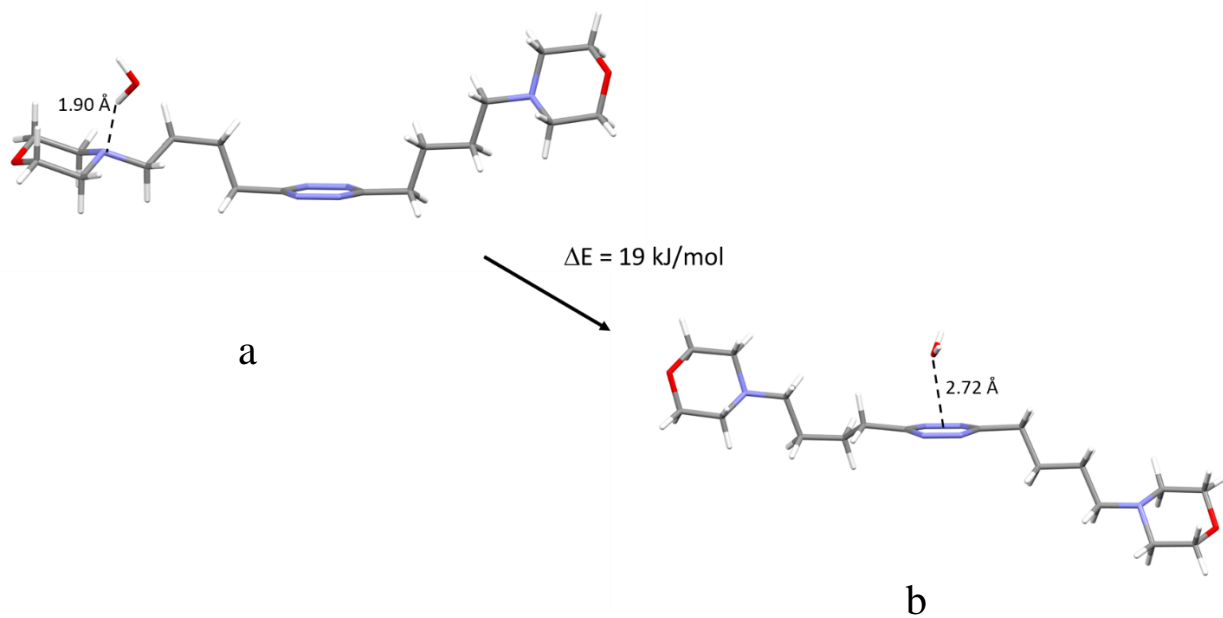


Figure S15. Calculated conformations for the $[L4(H_2O)]$ adduct: a) planar conformation, H-bond; b) planar conformation, lone pair- π .

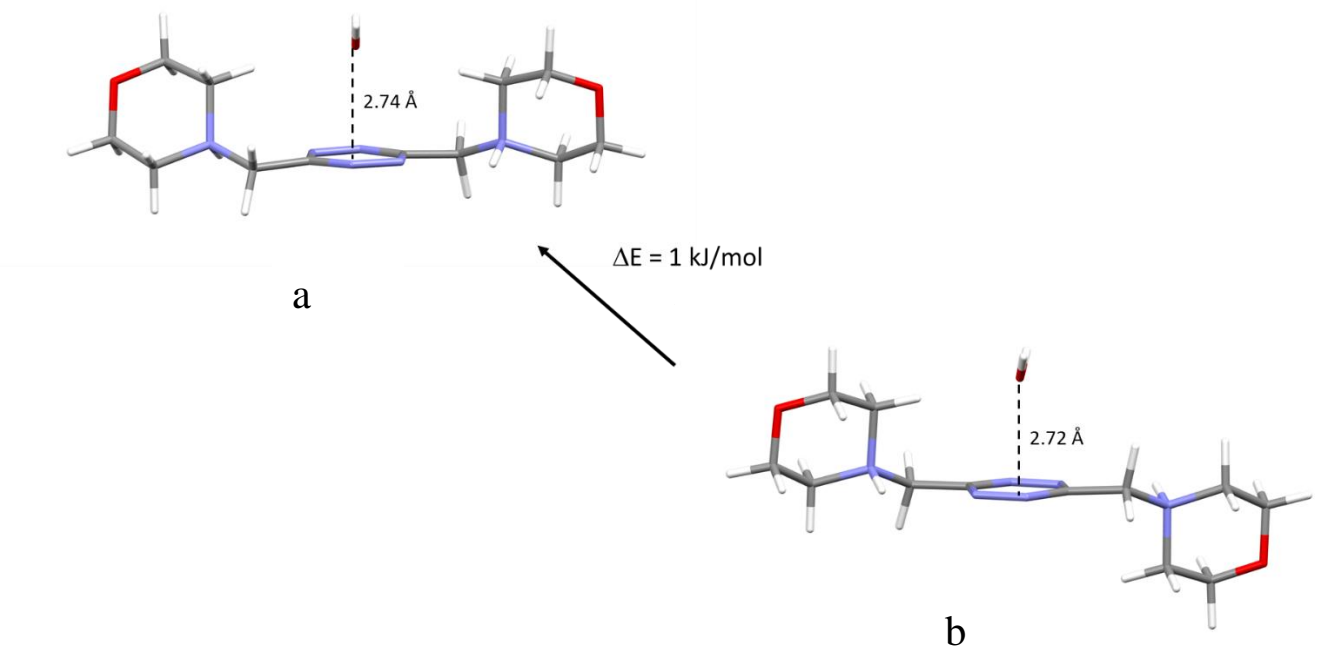


Figure S16. Calculated conformations for the $[\text{H}_2\text{L}1(\text{H}_2\text{O})]^{2+}$ adduct: a) boat conformation, b) chair conformation.

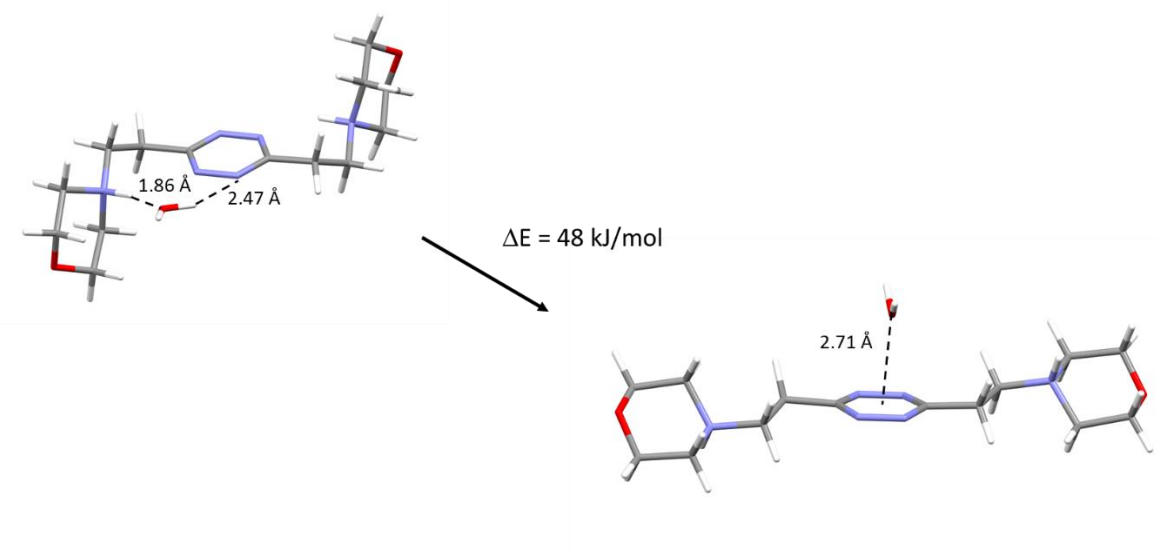


Figure S17. Calculated conformations for the $[\text{H}_2\text{L}2(\text{H}_2\text{O})]^{2+}$ adduct: a) chair conformation, b) planar conformation.

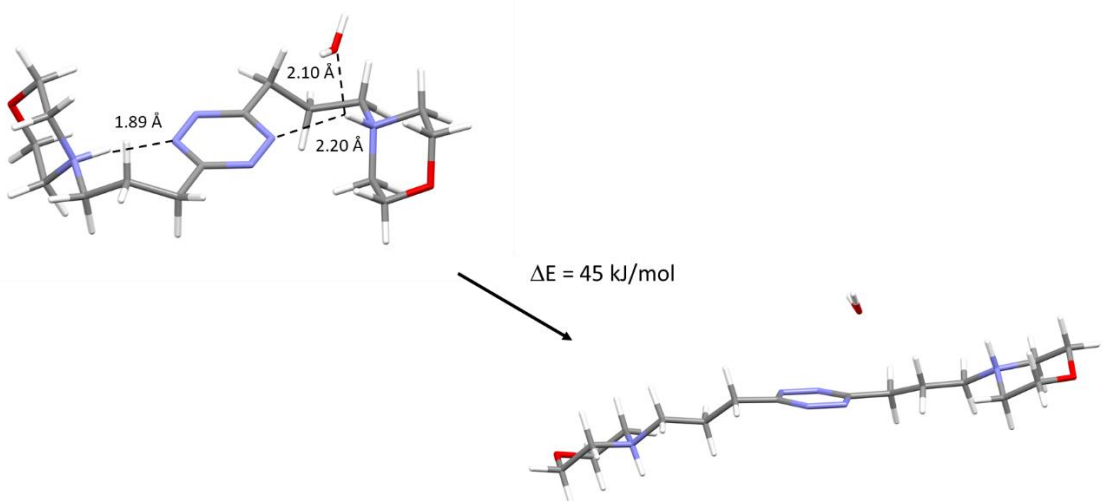


Figure S18. Calculated conformations for the $[H_2L3(H_2O)]^{2+}$ adduct.

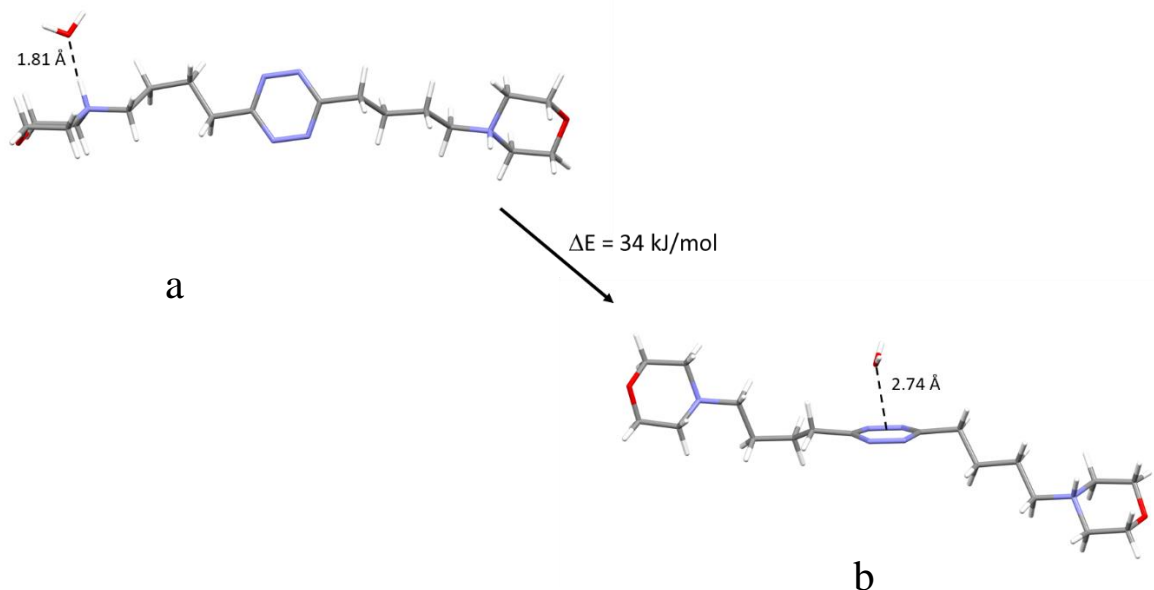


Figure S19. Calculated conformation for the $[H_2L4(H_2O)]^{2+}$ adduct: a) planar conformation, H-bond; b) planar conformation, lone pair- π .

L3 ClO₄⁻

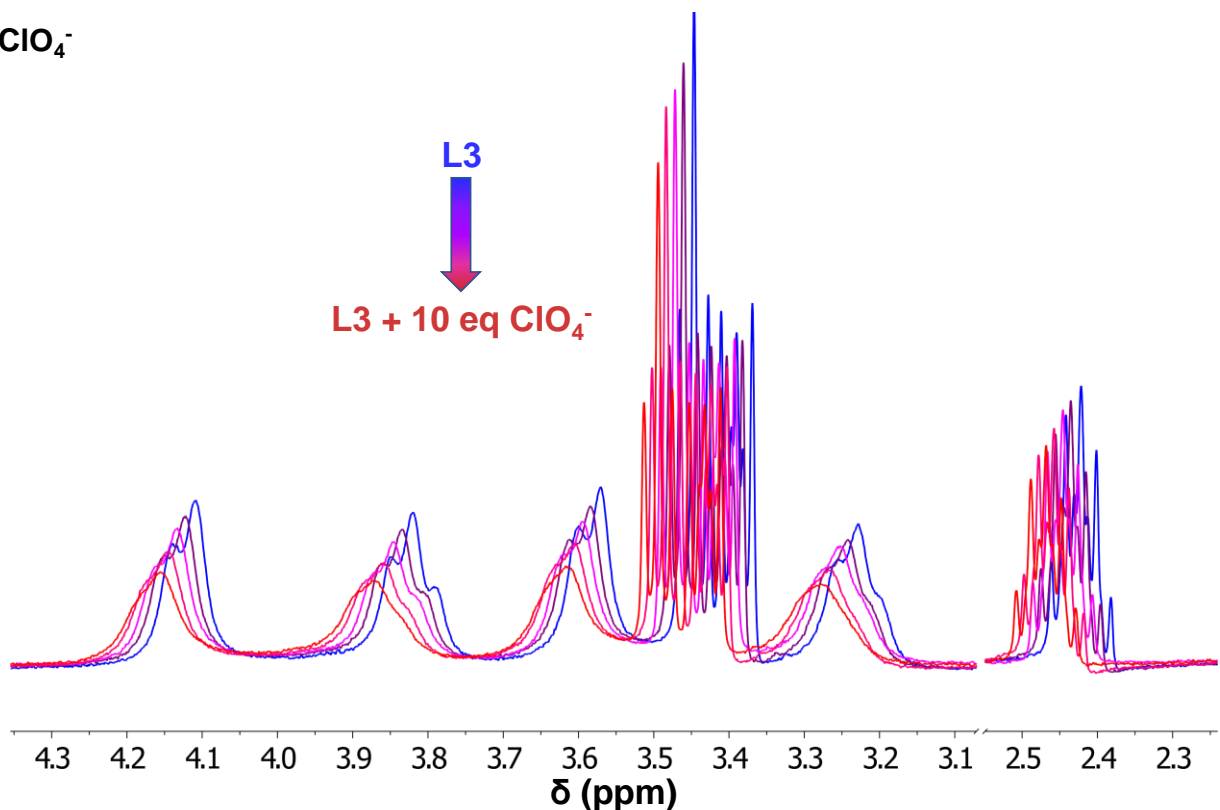


Figure S20. ¹H NMR spectra of L3 recorded in D₂O (pH 4) in the absence and in the presence of increasing amounts of ClO₄⁻.

L3 PF₆⁻

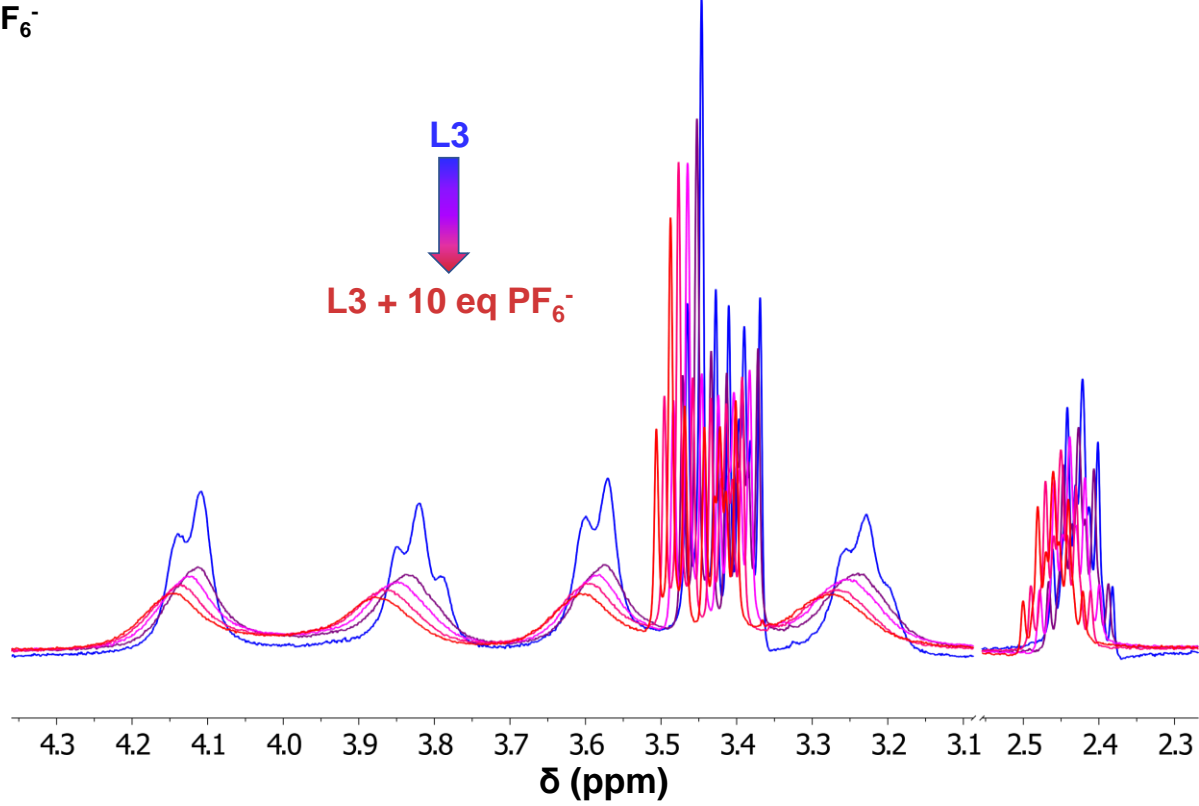


Figure S21. ¹H NMR spectra of L3 recorded in D₂O (pH 4)) in the absence and in the presence of increasing amounts of PF₆⁻.

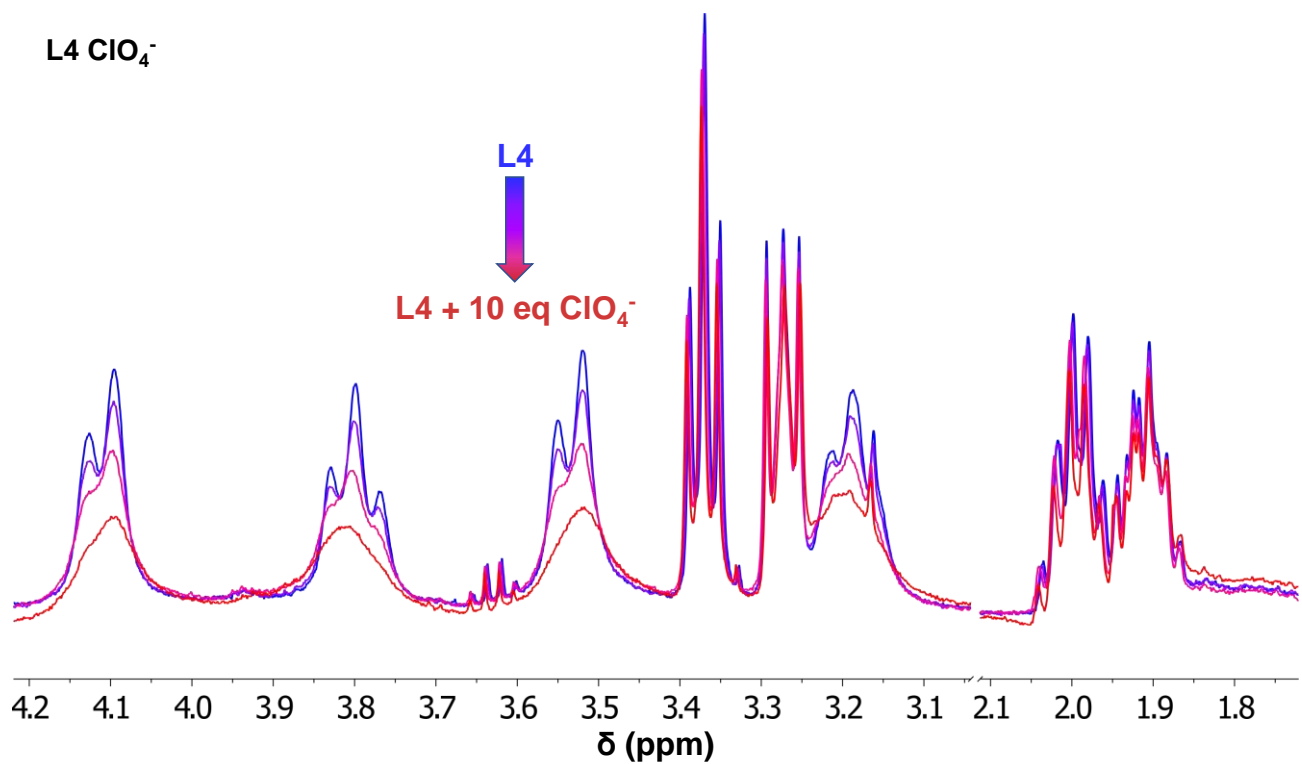


Figure S22. ^1H NMR spectra of L4 recorded in D_2O (pH 4) in the absence and in the presence of increasing amounts of ClO_4^- .

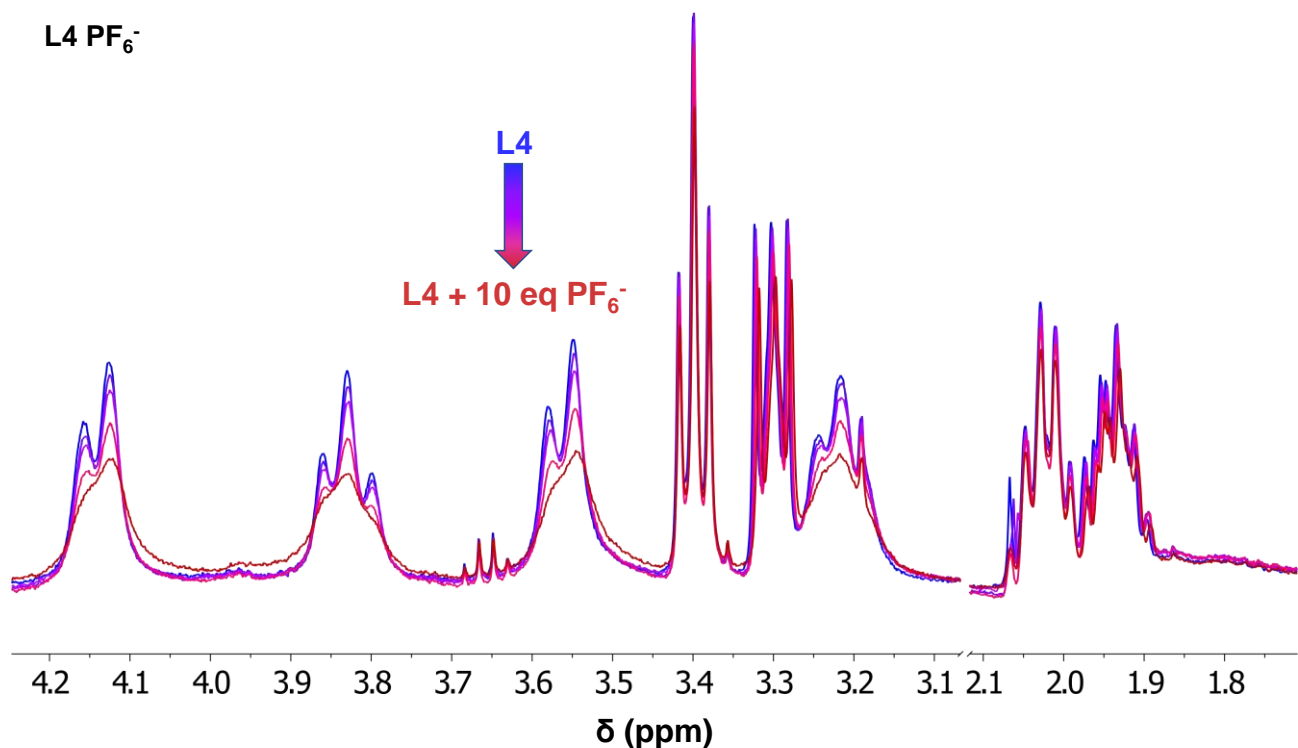


Figure S23. ^1H NMR spectra of L4 recorded in D_2O (pH 4)) in the absence and in the presence of increasing amounts of PF_6^- .